



Riverine landscape dynamics of the Upper Ganga River (Haridwar-Narora), India

Satish Prasad · Ridhi Saluja · Varun Joshi · J. K. Garg

Received: 28 July 2020 / Accepted: 11 January 2021 / Published online: 28 January 2021

© The Author(s), under exclusive licence to Springer Nature Switzerland AG part of Springer Nature 2021

Abstract Earth observation data provides an exceptional opportunity to study the temporal dynamics of large rivers. The availability of spatially continuous, synoptic and temporally repetitive satellite data allows the reconstruction of historical dynamics of large rivers along with the identification of the causal factors. An absolute paucity of information on the effect of hydrogeomorphic processes on the dynamics of the Upper Ganga River (UGR), especially upon its entry in the plains, motivated this research. This study aims to analyse morphological changes in the river channel, map temporal changes in the land use/land cover (LULC) within the riverscape and thereby understand the landscape dynamics in the UGR (Haridwar to Narora)

during 1993–2017 by means of earth observation data. The analysis showed that the river remains straight with a sinuosity index of < 1 ; however, the braiding increased considerably (from 3.79 to 4.53). Erosion being more prominent on the left bank in comparison to the right bank with 85.89 km² eroded on the left bank in comparison to 59.21 km² eroded along the right bank. Riverine landscape has been observed to have a higher rate of accretion in comparison to erosion (8.09 km² yr⁻¹ and 6.04 km² yr⁻¹, respectively). Morphological change has brought a transition in the land use patterns with marked variation in vegetation and agriculture along with built-up. Significant changes in the composition of the LULC are largely due to the manifold increase in the agriculture extent (≈ 12 times), built-up (5 times) and the decrease in vegetation cover from 43.9% in 1993 to just 10.94% in 2017.

S. Prasad (✉) · R. Saluja · V. Joshi · J. K. Garg
University School of Environment Management, Guru Gobind Singh Indraprastha University, Delhi, India
e-mail: sathshve12@gmail.com

R. Saluja
e-mail: saljarids@gmail.com
V. Joshi
e-mail: varunj63@gmail.com
J. K. Garg
e-mail: gargjk113@gmail.com

R. Saluja
Wetlands International South Asia, A-25, Defence Colony, New Delhi, India

J. K. Garg
Teri School of Advanced Studies, Vasant Kunj Institutional Area, New Delhi, India

Keywords Sinuosity · Braiding · Erosion-deposition · LULC · FRAGSTATS · River dynamics

Introduction

The riverbanks change continually in the transformation zone under the dynamic fluvial system acting as transitional boundaries connecting aquatic and terrestrial ecosystems (Florsheim et al. 2008). Hydrogeomorphic processes such as erosion, deposition, flooding and alteration of sediment load in a river system build, manage, and deteriorate the riverine landscape (Steiger et al. 2005). Similarly, sinuous and braiding pattern observed

in the transformation zone of rivers is an outcome of natural processes and sediment load (Leopold and Wolman 1957). A river's sinuosity is driven by of channel migration (Schumm and Khan 1972), where river flow-induced spatial patterns such as erosion-accretion are responsible for the change in curvature of the planform (Lazarus and Constantine 2013). Braiding is observed in rivers when its channel splits up around the sediment deposits or alluvial islands (Leopold and Wolman 1957), resulting from sediment load exceeding the rivers carrying capacity (Wang et al. 2016).

River patterns and processes are crucial for their management and conservation (Lovric and Tosic 2016). Besides, hydrogeomorphic studies provide guidance for the rehabilitation, conservation and management post commissioning of large-scale river projects such as construction of reservoirs, barrages and even irrigation canals (Langat et al. 2019). Alterations in the river course modify the land cover characteristics of the riverine landscape (Bhunia et al. 2016), thereby transforming the land use patterns. Changes in the LULC arising from river dynamics are in turn responsible for socio-economic and environmental challenges (Behera et al. 2012). Analysing changes in the land cover pattern within a known time frame is vital for understanding landscape dynamics and resource management thereof (Mondal and Mandal 2018). Moreover, a quantitative analysis of the dynamics of landscape patterns based on ecological indices is critical for riverine landscape conservation and management (Xiaofeng et al. 2009).

The conventional geomorphological investigation requires substantial investment (both financial and human resources) for in situ data collection, in addition to being time-consuming. Earth observation data overcomes the technical limitations of otherwise conventional methods providing a temporal aspect as well (Debnath 2017; Langat et al. 2019; Sudhakar and Sudhakar 2019; Wang et al. 2016). Several research studies have relied on earth observation data for exploring river channel changes and meander evolution (Bertalan et al. 2019), meandering geometry and channel shifting associated with LULC (Behera et al. 2014; Bhunia et al. 2016) and erosion-accretion and planform dynamics (Langat et al. 2019; Yao et al. 2013).

The Ganga River Basin (GRB) is one of the most extensive alluvial plains (Sinha et al. 2017), created by the world's most comprehensive sediment

dispersal system, carrying a remarkably large sediment load of 356 million tonnes per year (Khan et al. 2018). Being India's largest river, River Ganga has been studied to understand confluence dynamics (Roy and Sinha 2007), geomorphic diversity (Sinha et al. 2017), sinuosity (Dhari et al. 2014), braiding (Singh et al. 2019), changing channel courses (Rudra 2014), the evolution of planform morphology such as braiding and sinuosity index (Pal and Pani 2019) along with hazard of bank erosion (Thakur et al. 2012). Khan et al. (2018) modelled the sediment and flow dynamics of the Ganga River, employing multiple climate change scenarios. Sinha et al. (2017) documented the geomorphic diversity and complexity of the Ganga River system at the reach scale. Using the Dyna-CLUE model, Behera and Behera (2020) predicted the pattern of land use and land cover in the GRB for year the 2045. Mukherjee et al. (2017) examined the erosion and deposition along the river banks for 91 years using GIS in the lower Ramganga River. Rudra (2010) studied fluvial dynamics in the lower reach of river Ganga for 240 years. Gupta et al. (2013) evaluated the decadal length changes in the fluvial planform near Farakka Barrage in River Ganga using satellite imagery. There is no specific study that monitored LULC change in the Upper Ganga River landscape, but Flint (2002) observed the changes from 1880 to 1980 in LULC over the Gangetic Plain. The cultivated area increased from 33.9 to 39.9 M ha by 17.3%, while the built-up area in the Gangetic Plain increased enormously from 12.1 to 132.3%. By contrast, forest cover decreased by 40% (0.6 M ha), and wetlands lost nearly half of their area in the past century. The population density of the region increased by 176% during the same period.

Although several research studies have focused on the dynamics of River Ganga, there is an absolute paucity in terms of efforts made to understand the interrelationship between hydrogeomorphic processes and the land use pattern in the UGR. Thus, the existing lacuna and ecological significance of Upper Ganga River necessitate an assessment of dynamics to further its conservation and monitoring. This study therefore aimed at (i) analysing morphological changes in the UGR, (ii) assessing changes in land use land cover due to river dynamics, and (iii) investigating the relationship between LULC changes and river dynamics using landscape metrics.

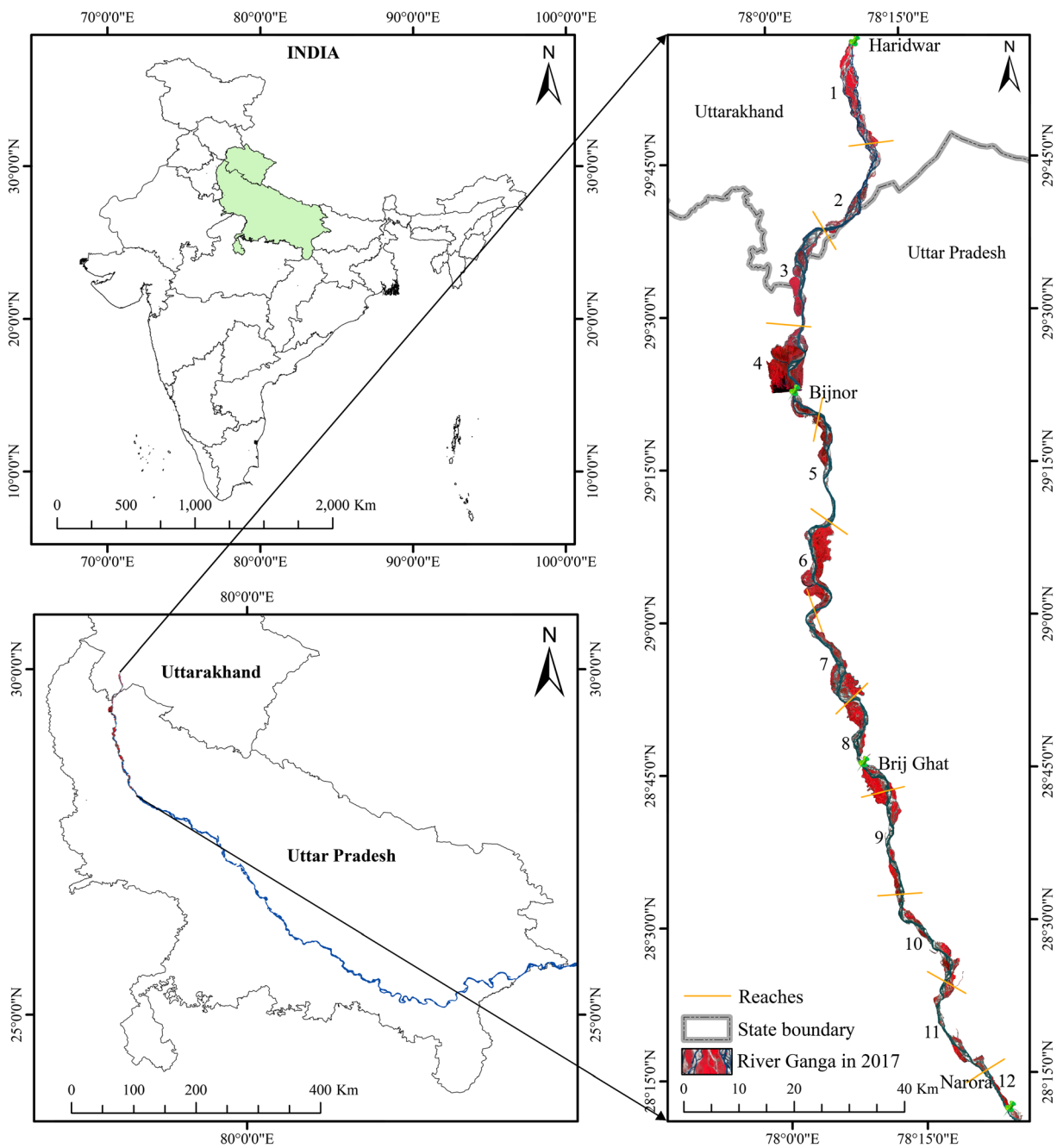


Fig. 1 Location map of the study area

Materials and methods

Study area

River Ganga is a glacier-fed river that originates from small streams and melting glacial ice at an altitude of 6000 m in the state of Uttarakhand, India (Sanghi and Kaushal 2014).

The headwater of river Ganga encompasses countless small rivulets arising in the Himalayas. However, the six largest tributaries, Alaknanda, Dhauliganga, Nandakini, Pindar, Mandakini, and Bhagirathi, together take the form of the River Ganga (Tare et al. 2015). After eroding the mountainous terrain for several hundred kilometres, River Ganga enters the Indo-Gangetic plain at Haridwar

(Bandyopadhyay 1995). The study area extends from the holy city of Haridwar, in Uttarakhand (78° 03' E, 29° 35' N) to Narora in the state of Uttar Pradesh (78° 25' E, 28° 47' N) covering a distance of 240 km (Fig. 1) including the Upper Ganga River (Brijghat to Narora), a wetland of international importance or a Ramsar site (Ramsar 2005). By and large, the Indo-Gangetic plain was formed as an after effect of the continent-continent collision in the early Miocene. Over the arched Indian plate, the alluvial plain expanded during the Middle Miocene and reached its present state in the Late Quaternary (Singh 1996). Riverine landscape after the River Ganga enters the alluvial plains (Haridwar to Bijnor) is piedmont composed of unconsolidated sand, silts with/without clay piedmont, partially confined floodplains and braided channels (river class III) (Sinha et al. 2017). Furthermore, the Bijnor-Narora landscape is characterized by central alluvial plain, valley-interfluve, partially confined floodplain and braided channels (river class IV) (Sinha et al. 2017). As observed during 1880, Tian et al. (2014) characterized the Gangetic Plain by grasslands, shrubland and fallow land use type, since any known forest or less known forest area was already cleared before 1893 in the riverine landscape (Richards and Flint 1994). This section of the river is now highly cultivated and industrialized marked by predominance of sugar, pulp, paper, chemicals and leather industries along with distilleries (Chaudhary et al. 2017; CPCB 2013).

Image processing and river delineation

Channel dynamics within the UGR was analysed using temporal Landsat imagery. In order to minimize the cloud coverage and ensure error-free delineation of the river stretch, post-monsoon Landsat imagery for the month of October representing year 1993 and 2017 was downloaded from USGS Earth Explorer tool. Satellite images were radiometrically and atmospherically corrected to extract the top-of-the-atmosphere (TOA) reflectance. In a multi-step process, the radiometric correction transformed digital number (DN) to radiance, following which the atmospheric correction using the Fast Line-of-sight Atmospheric Analysis of Spectral Hypercubes (FLAASH) system transformed radiance to TOA reflectance in Environment for Visualizing Images (ENVI) version 5.3 (Exelis Visual Information Solutions, Boulder, CO, USA) software.

The river was extracted from the satellite imagery using a binary mask generated using a decision tree built using spectral band reflectance (SWIR 1; 1.57–

1.65 μm) and modified normalized difference water index (MNDWI) (Xu 2006). In addition, various band combinations were used to accurately extract the river channel boundary (7, 5 and 4 for Landsat 8 and bands 5, 4 and 3 for ETM+). River boundary was then corrected based on visual interpretation and rectified via heads-up digitisation at a constant scale of 1:1000, and the entire process was performed by a single operator to ensure precision. Digitization was performed at a small scale as it ensures accuracy in capturing details related to river (Rozo et al. 2014). For further analysis, the river stretch was divided into 12 equal reaches (equivalent to a length of 20 km) (Fig. 1).

Fluvial geomorphology

Sinuosity and braiding

Sinuosity index is the ratio of the length of the river measured along the river's thalweg line to the horizontal distance between the channel's starting and ending points in a river's reach (Ozturk and Sesli 2015). A modified approach outlined by Friend and Sinha (1993) was used to calculate the sinuosity for the river stretch. It is the ratio of centreline length of a major channel, and the horizontal distance between the start and end point of the reach analysed (Eq. 1) (Dhari et al. 2014; Ozturk and Sesli 2015):

$$S = \frac{L_{c \max}}{L_0} \quad (1)$$

where $L_{c \max}$ is the centreline length of the major/widest channel of the reach and L_0 is the overall length of the reach.

Table 1 LULC classes identified within the riverine landscape

Class name	Description
Agriculture	Area under cultivation (standing crop)
River	River Ganga/river channel
Sandbar	Sandy area in the river channel and riverscape
Bare soil	Barren area or not having vegetation and crop, but not sandy
Vegetation	Mixed sparse vegetation and/or herbaceous (scrub)vegetation
Built-up	Urban and rural continuous and discontinuous areas

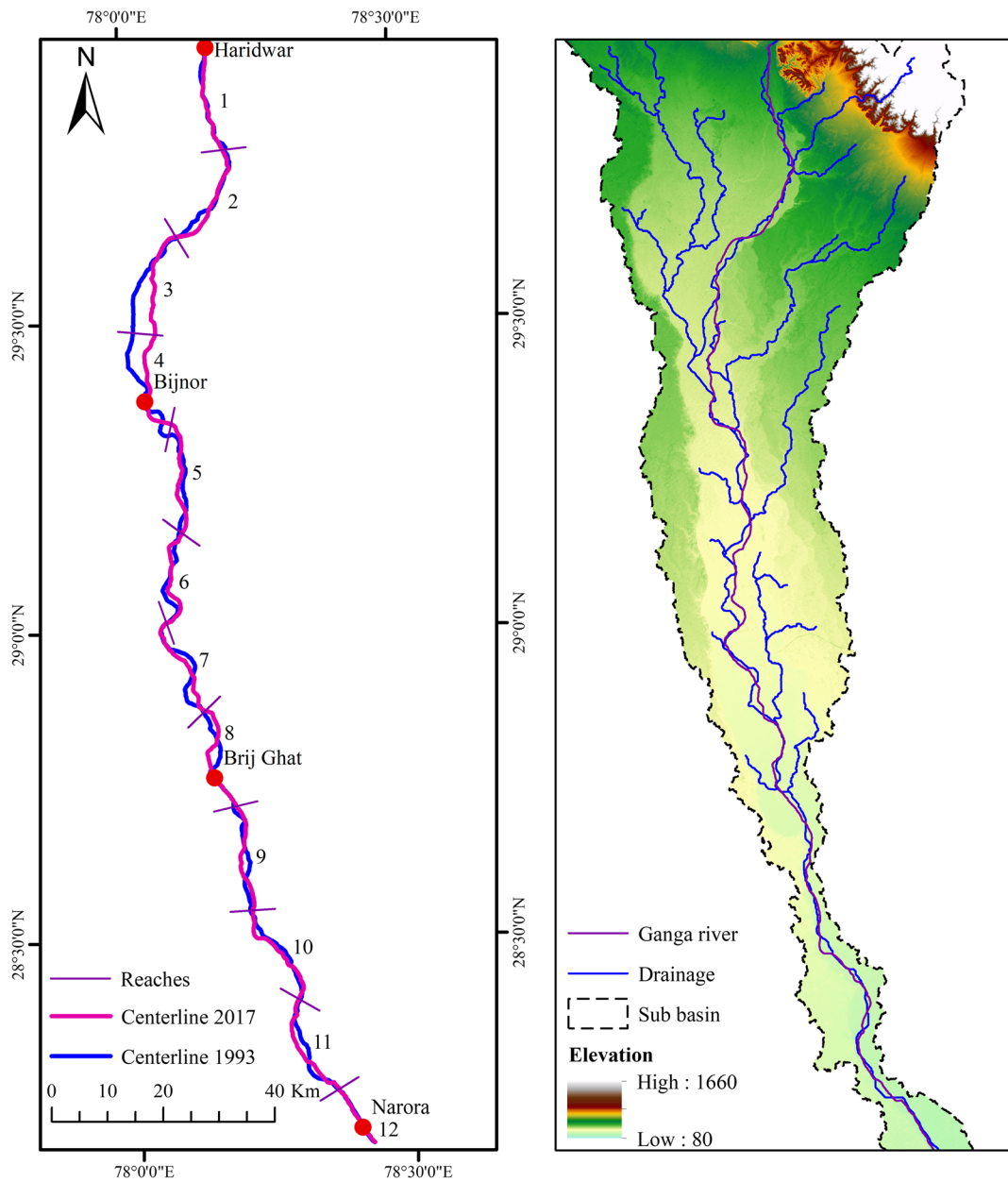


Fig. 2 Comparison of river centreline and river in the landscape

Braiding was calculated based on Saikia et al. (2018) using a fraction of area covered by sandbars, number of bars in mid-channel and maximum width of the reach to calculate braiding index (Eq. 2):

$$B = X \times N^* \times \frac{W}{L} \tag{2}$$

where X = fraction of area covered by bars, N^* = number of bars in mid-channel, L = length of reach and

W = maximum width of the reach. The river stretch was then classified based on Saikia et al. (2018) as highly braided ($B > 30$), moderately braided ($5 < B < 30$) and low braided ($B < 5$).

Erosion and deposition

Erosion and deposition patterns along the banks of the UGR were analysed in GIS environment for the years

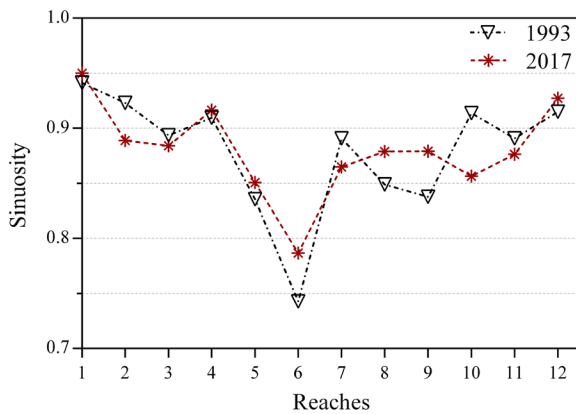


Fig. 3 Sinuosity in different reaches during 1993 and 2017

1993 and 2017. Analysis was based on the method applied by Langat et al. (2019) and Saleem et al. (2019) for estimating erosion and deposition in Tana River, Kenya and Padma River in Bangladesh, respectively.

LULC classification

Six land use land cover classes were identified in the riverine landscape to determine changes in LULC during period 1993–2017 (Table 1). Landsat imagery was analysed using supervised classification with maximum likelihood algorithm in ERDAS Imagine 14.0 following Bhunia et al. (2016), Debnath (2017)) and Saikia et al. (2019). Using high-resolution imagery from Google Earth and in situ data, 100 random polygons for each

Table 2 Braiding index (*B*) for 1993 and 2017

Reach number	Braiding (1993)	Braiding (2017)
1	6.40	7.96
2	3.58	2.98
3	9.37	2.63
4	1.81	10.37
5	2.17	0.85
6	4.39	5.68
7	2.48	8.12
8	4.68	6.83
9	5.41	5.25
10	0.76	1.82
11	4.02	1.13
12	0.42	0.73
Total river stretches	3.79	4.53

LULC class were delineated as input training dataset. Classification using maximum likelihood classification (MLC) algorithm takes into account the reflectance value of each class in each band, in order to determine the probability of the given pixel belonging to a particular LULC class. The accuracy of classification performed was assessed using ground truth data (50 random reference point for each class) through confusion matrix (Bhunia et al. 2016; Debnath 2017).

Landscape pattern analysis

Landscape indices facilitate an easy understanding of how the landscape under study modified over a selected period of time while identifying areas that have undergone transformation while facilitating determination of underlying cause of change and streamlining patterns. In this study, landscape metrics were analysed at class and landscape level using FRAGSTATS (v 4.3) developed by McGarigal et al. (2012) and were used by various researchers to study landscape dynamics in a mountainous river basin of India (Gaur et al. 2019), similarly used by Lamine et al. (2018) and Zhang et al. (2015) to analyse the spatio-temporal dynamics of LULC in a Mediterranean ecosystem and middle reached of Tarim river, respectively. To characterize the landscape pattern at class level, five metrics were calculated, namely, (a) area and perimeter metrics (AREA (ha), mean patch area (AREA_MN), largest patch index (LPI, %) and percentage of like adjacencies (PLAND, %)); (b) aggregation metrics (number of patches (NP) and patch density (PD, patches/100 ha)); (c) distance metrics (Euclidean nearest neighbour (ENN_MN, m)); and (d) fragmentation metrics (effective mesh size (MESH, ha)). For the analysis, the cell size was 30 m, and 8 cell neighbourhood rule was applied for patch neighbours.

Results

Assessing fluvial geomorphology of the Upper Ganga River

Extent of the UGR decreased by 3.87 km during the study period from 239.6 to 235.73 km. Figure 2 shows a comparison of the river centerline for the years 1993 and 2017. To understand the effect of Bijnor and Narora barrages on sinuosity and braiding, the river was analysed within 12 reaches. Reach 1 had the maximum

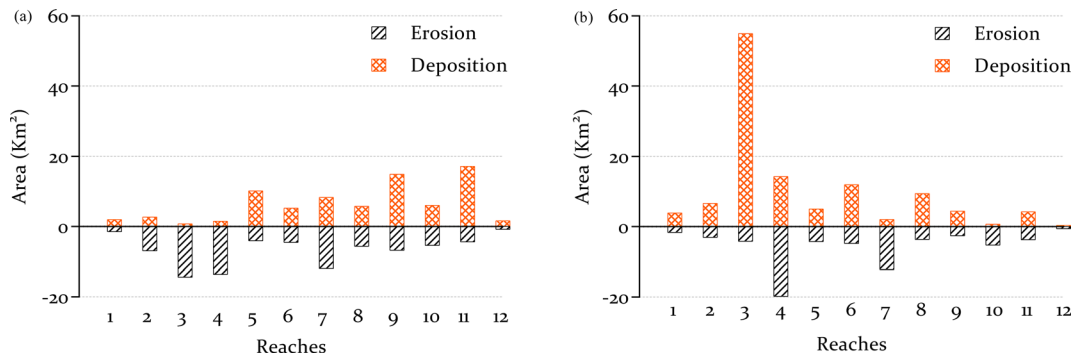


Fig. 4 Bank erosion and deposition in different reaches of the UGR, during 1993–2017: **a** left bank and **b** right bank

sinuosity value of 0.94 for both years, whereas the minimum sinuosity values were observed at reach 6 (0.74 and 0.78 in 1993 and 2017, respectively). The results show that the river stretch is within the sinuosity index value of < 1 for the entire study area (Fig. 3), suggesting that the river has not meandered much and remained more or less straight. This can be attributed to the gradual decrease in the elevation from the Gangetic Plain (Haridwar) entry point to the Narora.

Variation in braiding index along the reaches of the UGR are shown in Table 2 and Supplementary Table S1 and Supplementary Table S2. Because of the presence of a barrage, braiding values for reach number 12 were the lowest (0.42 and 0.72 for 1993 and 2017 respectively). Reaches 1, 3 and 9 were moderately braided, while all other reaches were less braided for 1993 with a

maximum braiding value observed at reach 3 ($B = 9.37$). In 2017, reaches 1, 4, 6, 7, 8 and 9 were moderately braided, and all other reaches were low braided, while the maximum braiding among the reaches was observed at reach 4 ($B = 10.36$). An overall increase in braiding index was observed from the year 1993 to 2017 (3.79 to 4.53, respectively).

Erosion and deposition in the river are highly dependent on flow, volume and sediment load. Bank erosion and deposition influence changes in the river morphology. The dynamic changes arise due the process of erosion and deposition. High variability has been observed in erosion and deposition over the river stretch temporally as well as spatially during the study period. Areal extent of erosion and deposition during 24 years on the

Table 3 Rate of bank erosion and deposition for the Upper Ganga River

Reach	Erosion rate (km ² yr ⁻¹)			Deposition rate (km ² yr ⁻¹)		
	Overall rate	Left bank	Right bank	Overall rate	Left bank	Right bank
1	0.13	0.06	0.07	0.24	0.08	0.16
2	0.41	0.29	0.13	0.39	0.11	0.28
3	0.77	0.6	0.17	2.32	0.03	2.29
4	1.39	0.57	0.82	0.66	0.06	0.6
5	0.35	0.17	0.18	0.63	0.42	0.21
6	0.39	0.19	0.2	0.72	0.22	0.5
7	1.00	0.5	0.51	0.43	0.35	0.08
8	0.39	0.24	0.15	0.63	0.24	0.39
9	0.39	0.28	0.11	0.81	0.62	0.18
10	0.44	0.22	0.22	0.28	0.25	0.03
11	0.34	0.18	0.15	0.89	0.72	0.18
12	0.05	0.03	0.02	0.08	0.07	0.01
Total river stretches	6.05	3.32	2.72	8.09	3.17	4.92

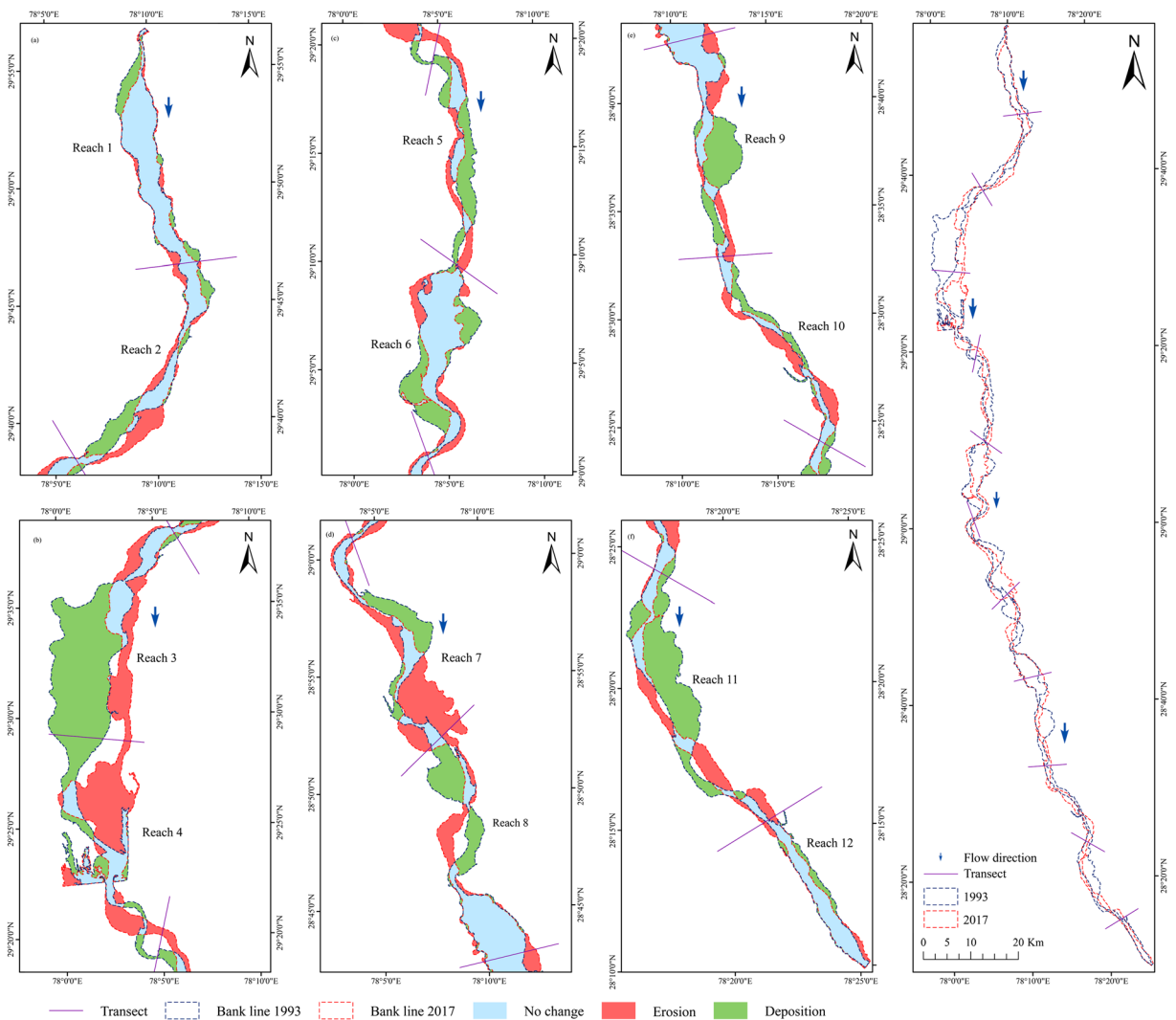


Fig. 5 Erosion and deposition for different reaches during 1993–2017 in the Upper Ganga River

river’s left and right bank at different reaches is shown in Fig. 4. The left bank eroded 85.89 km² as compared to 59.21 km² along the right bank. However, the deposition was more prominent on right bank than the left bank (117.98 and 76.17 km², respectively). It is interesting to note that the erosion on the left bank gradually decreases downstream while deposition increases. However, on the right bank, this is not the case; the erosion and deposition peak at reaches 3 and 4 and then gradually decline downstream. The gradual decline in the erosion can be attributed to the decrease in flow and presence of barrages at Narora and Bijnor (Sanghi and Kaushal 2014) and also due to the increase in sediment load as

the overall sediment load of river increased from 329 Mt yr⁻¹ (Subramanian 1996) to 356 Mt yr⁻¹ (Khan et al. 2018). Highest erosion was observed at reach 4 with 19.73 km² on the right bank and the highest deposition of 54.97 km² on the right bank at reach 3. However, it is interesting to note that the total area deposited was more as compared to the area under eroded (194.166 and 145.107 km², respectively).

Deposition rate (8.09 km² yr⁻¹) was higher than the rate of erosion (6.04 km² yr⁻¹) for the study area. The erosion rate at the left bank was higher than at the right bank (3.32 and 2.72 km² yr⁻¹, respectively). In contrast, the deposition rate in the right bank was much higher than in the left bank (4.92 and 3.17 km² yr⁻¹, respectively) (Table 3).

Table 4 Number and area of plots at different reaches in left and right bank of the UGR from 1993 to 2017

Reaches	Erosion							
	Left bank				Right bank			
	No. of plots	Area (km ²)			No. of plots	Area (km ²)		
		<1	1–10	>10		<1	1–10	>10
1	18	18			36	36		
2	7	6	1		17	16	1	
3	3	2		1	1		1	
4	24	22	1	1	55	52	2	1
5	8	6	2		8	5	3	
6	5	4	1		12	11	1	
7	7	5	1	1	6	3	3	
8	10	8	2		26	25	1	
9	4	1	3		27	27		
10	5	3	2		31	29	2	
11	5	2	3		13	11	2	
12	14	14			52	52		
	Total plots=110	91	16	3	Total plots=284	267	16	1
Reaches	Deposition							
	Left bank				Right bank			
	No. of plots	Area (km ²)			No. of plots	Area (km ²)		
		<1	1–10	>10		<1	1–10	>10
1	21	20	1		23	23		
2	11	10	1		17	16	1	
3	2	2			2	1		1
4	21	21			43	38	5	
5	1		1		5	3	2	
6	4	3	1		7	5	2	
7	5	4	1		5	4	1	
8	9	8	1		24	23	1	
9	3	1	1	1	21	21		
10	6	4	2		13	13		
11	3	1	1	1	13	11	2	
12	15	14	1		48	48		
	Total plots=101	88	11	2	Total plots=221	206	14	1

Figure 5 shows the area of erosion, deposition and no change within the bank lines for the years 1993 and 2017. The unification of bank lines for both years shows that this stretch of the UGR has significantly shifted its bank line over the years, causing a loss in arable land and habitat.

Bank line analysis revealed 110 plots of erosion on the left bank and 284 plots of erosion on the right bank (Table 4). The left bank had three plots with substantially large area (> 10 km²), while the right bank had only one

plot larger than 10 km². The right bank had more plots (267 plots) than the left bank (91 plots) smaller than 1 km². Both banks had an equal number of plots between 1 and 10 km². Bank line analysis for deposition shows similar trends with more plots on the right bank than on the left bank (221 and 101 plots, respectively). The right bank had more than double the number of plots (206) compared with the left bank (88) of less than 1 km². The left bank had 2 plots, and the right bank had only one plot greater than

Table 5 Land use land classes of the UGR during 1993 and 2017

Reaches	Area (km ²)						
	Agriculture	River	Sandbar	Bare soil	Vegetation	Built-up	Total
1993							
R1	2.23	11.08	6.60	14.56	21.43	0.02	55.93
R2	17.96	12.67	6.34	24.41	55.41	1.11	117.89
R3	5.53	13.92	10.25	17.77	69.84	0.19	117.50
R4	0.06	18.76	3.67	3.32	50.61	0.04	76.45
R5	0.05	8.09	7.42	10.94	11.56	0	38.05
R6	0.01	9.10	6.86	7.82	29.47	0	53.26
R7	0.05	10.36	6.89	12.89	12.22	0	42.40
R8	0.03	11.26	10.74	12.95	12.31	0.06	47.33
R9	0.02	10.23	12.65	16.53	7.55	0	46.97
R10	0	9.38	6.69	4.73	7.75	0	28.55
R11	0	10.76	4.49	4.43	11.86	0	31.55
R12	0.00	6.19	1.72	0.55	3.28	0.05	11.79
Total river stretches	25.93	131.77	84.32	130.88	293.28	1.46	667.64
2017							
R1	8.87	11.66	3.91	15.32	15.82	0.81	56.38
R2	70.63	14.09	3.13	14.24	18.97	4.01	125.06
R3	93.47	16.90	1.80	10.38	2.66	1.29	126.50
R4	26.93	18.94	1.03	11.52	27.56	0.06	86.03
R5	8.29	11.07	1.02	5.79	0.06	0	26.23
R6	36.65	11.74	1.09	9.69	2.27	0	61.44
R7	15.40	12.89	0.92	14.10	0.47	0	43.77
R8	20.97	13.02	1.03	11.31	0.67	0.08	47.06
R9	14.28	10.38	1.48	7.10	0.83	0	34.06
R10	7.95	10.80	1.59	10.95	1.74	0	33.04
R11	5.00	9.11	1.14	9.55	2.73	0.06	27.58
R12	2.07	5.28	0.86	3.01	0.55	0.10	11.86
Total river stretches	310.49	145.88	18.98	122.96	74.31	6.40	679.01

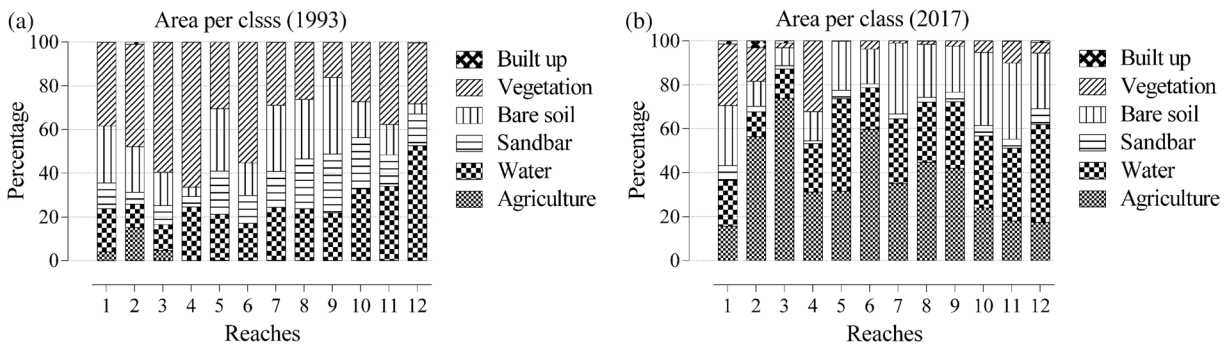


Fig. 6 LULC area under each class

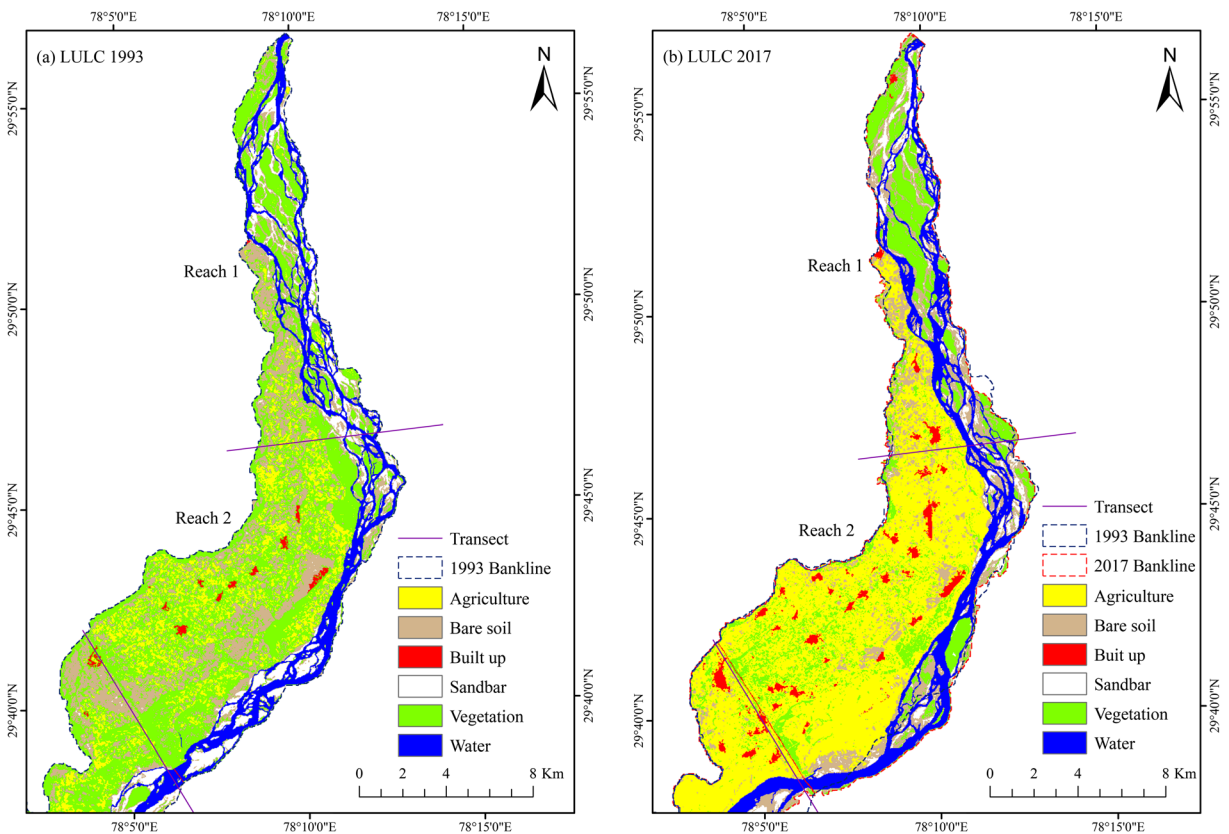


Fig. 7. L. ULC maps from Landsat series images **a** 1993 and **b** 2017 using MLC classification for reaches 1 and 2

10 km². Compared with the deposition, there are more erosion plots of an area greater than 10 km². Prevalence of erosion plots suggest that although the deposition was higher than erosion, during the study period, the river shows increased braiding and fragmentation.

Landscape configuration and temporal change

The assessment of land use land cover changes presents a plausible understanding of the UGR’s erosion and deposition characteristics. Erosion and deposition along the river channel dictate the changes in the landscape dynamics. The dynamic nature of the Ganga River has been studied mostly in the delta and lower Ganga region (Bhaskar et al. 2012; Gupta et al. 2013; Rudra 2010; Thakur et al. 2012), with the upper region of the Ganga River under analysed.

Table 5 and Figs. 7, 8, 9, 10, 11 and 12 show the transformation of LULC in the UGR from 1993 to 2017. In 1993, an area of 25.93 km² was under agriculture with River Ganga occupying 131.77 km². Sandbar

occupied an area of 84.32 km², while bare soil in the riverine landscape covered an area of 130.88 km². Vegetation dominated the land cover in 1993 covering (293.28 km²; 43.9%), and built-up was restricted to only 1.46 km² (0.22%) of the landscape (Fig. 6).

The LULC analysis of the UGR revealed that the study area has undergone radical changes. The overall classification accuracy for 1993 was 92.58% and 96.48% for 2017 (Supplementary Table S3) with the kappa coefficient value of 0.90 (1993) and 0.95 (2017).

Marked alterations were mapped in 2017 as compared to 1993. The area under agriculture increased multifold (≈ 12 times) to occupy maximum area (310.49 km²), and the built-up increased five times to cover 6.40 km² of the landscape. River Ganga and bare soil occupied an area of 145.88 and 122.96 km², respectively, and the sandbar area decreased to 18.98 km². Loss of vegetation was highly evident from 1993 to 2017 (293.28 km² to 74.31 km², respectively, Table 5).

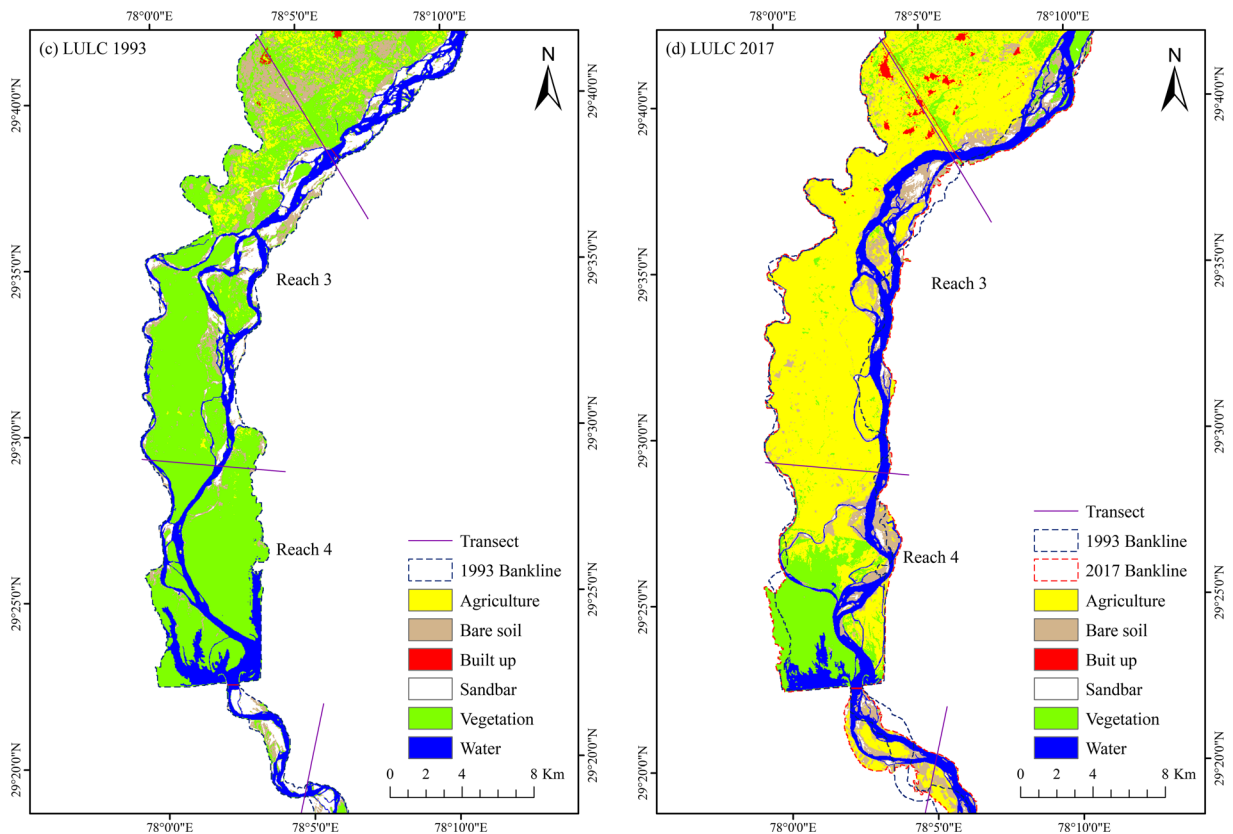


Fig. 8 LULC maps from Landsat series images **c** 1993 and **d** 2017 using MLC classification for reaches 3 and 4

Thus, the marked change in the LULC composition is largely attributable to conversion of vegetation from 43.9% in 1993 to just 10.94% in 2017. Majority of the area under vegetation was converted to agricultural area (45.72% in 2017 from 3.88% in 1993). River Ganga accounted for 21.48% of the total area, while built-up and sandbar accounted for 0.9% and 2.79% respectively.

Ecological indices

In 1993, the maximum percentage of landscape (PLAND) was occupied by vegetation (43.9%), with built-up (0.21%) occupying minimum land proportion, but in 2017, the maximum PLAND was observed in agriculture (45.68%), and built-up (0.94%) occupied the least PLAND (Table 6). PLAND results explicate that vegetation dominated the region; however, the trend points towards the gradual decline, as agriculture was the dominant cover type in 2017. The maximum number of patches for both years was observed for bare soil cover type (7670 and

5479 in 1993 and 2017, respectively). In 1993, the minimum NP was observed for built-up (value = 27), and in 2017, the river had the least NP (value = 47). A decrease in the total number of patches (17,845 in 1993 and 13,657 in 2017) and PD (26.74 and 20.13 number/100 ha in 1993 and 2017, respectively) indicates decreased fragmentation.

However, it means a decrease in the region's heterogeneity and an increase in the dominance of homogeneous patch leading to depletion in the riverine landscape's available habitat. The LPI was maximum for vegetation (11.29%) in 1993 and agriculture (25.37%) in 2017, indicating the shift in dominance of land cover type. It is suggestive that over the period, the homogeneous patches of agriculture dominate the region. In comparison to 2017, value of ENN_MN for the built-up class is higher during the year 1993, indicating a decrease in patch isolation, which means that the interpatch distance between the built-up class has decreased. Similar trend has been observed for agriculture as well. However, the interpatch distance increased for vegetation class, indicating fragmentation.

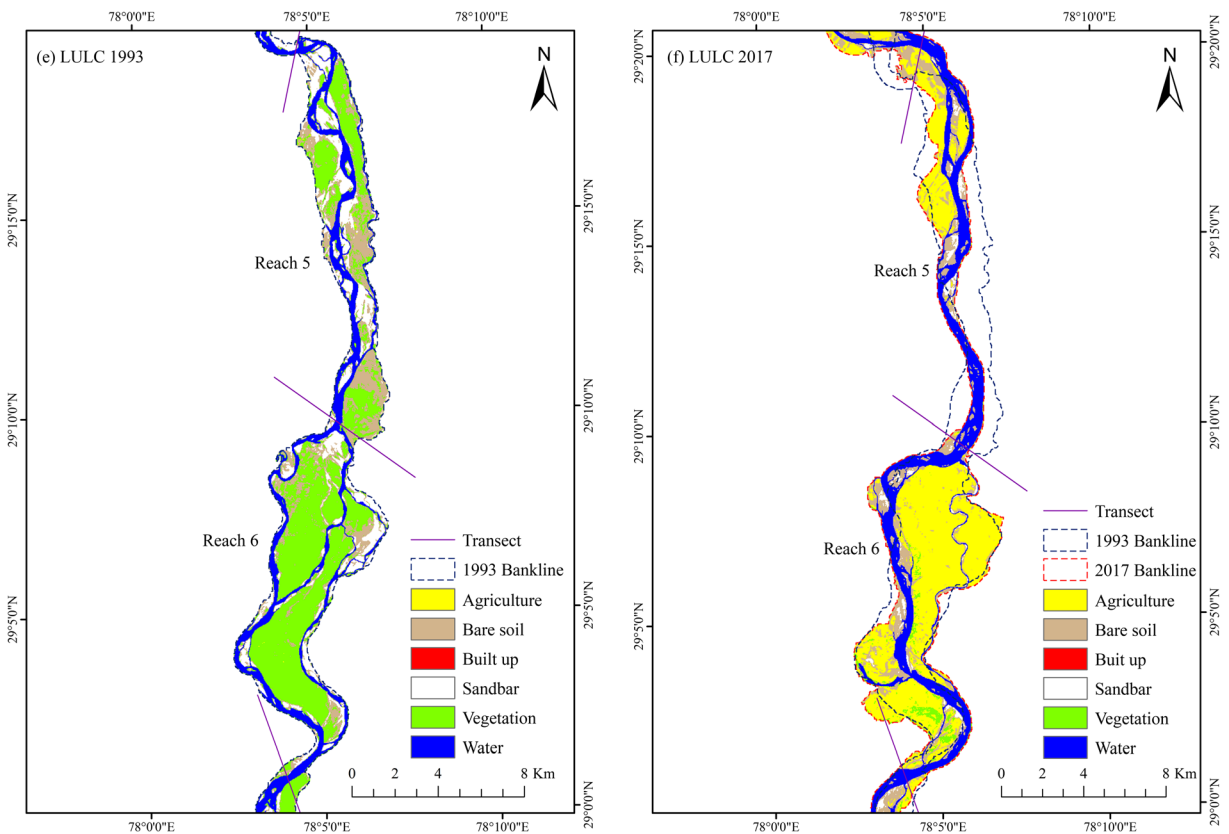


Fig. 9 LULC maps from Landsat series images **e** 1993 and **f** 2017 using MLC classification for reaches 5 and 6

Discussion

Rivers are dynamic as they adapt horizontally or vertically to changes in their bulk load and flow rate (Mukherjee et al. 2017). Dragičević et al. (2017) acknowledge that investing in the monitoring of channel shifts, erosion and deposition are economically conducive endeavours compared to remediating damage and loss of resources. The Ganga River is a large alluvial river carrying high volumes of sediment and water, with anthropogenic and natural events altering its configuration.

Rivers originating in the Himalayas are confined to the mountainous terrain and, due to their flow rate and sediment load, the planform characteristics of the rivers change when they enter the alluvial plains. For both the years observed, the Upper Ganga River was comparatively straight and moderately braided, with the mean sinuosity of 0.87 attributed to the confined channels and the barrages built at Bijnor and Narora (Singh et al. 2019). Roy and Sinha (2018) also observed the

sinuosity of the Ganga river, ranging between 1 and 1.32, attributing to its confined channels. Similar results were observed by Dhari et al. (2014) for the river Ganga (Haridwar-Balawali, Uttarakhand). As the geomorphic characteristics of the river planform are mainly regulated by flow, sediment transport and direct interference in the river channel are due to anthropogenic interventions (Roy and Sinha 2018). The river discharge is closely associated with spatial changes in channel planform. The variables that drive changes in discharge, particularly in the Upper Ganga River, are seasonal precipitation and flow alterations mediated by barrage construction at Bijnor and Narora.

During 1993 and 2017, the stretch of Upper Ganga River was classified as low to moderately braided. However, in 2017, a more significant number of reaches were classified as moderately braided compared to 1993, suggesting an increased braiding of the river. Moreover, during the study period, the mean braiding index increased from 3.79 to 4.53. Low sinuosity and rising braiding index values during the investigation

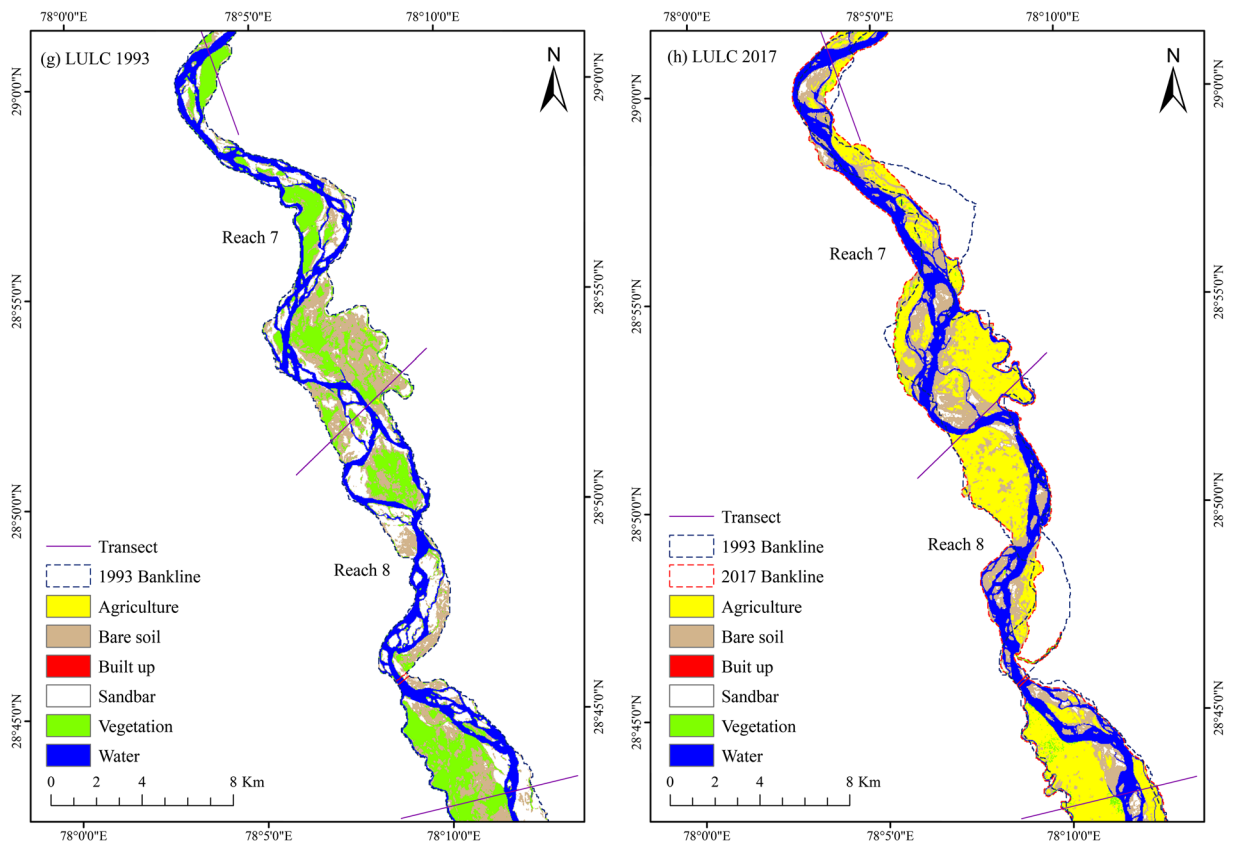


Fig. 10 LULC maps from Landsat series images **g** 1993 and **h** 2017 using MLC classification for reaches 7 and 8

period signify an amplification of sediment supply (Friend and Sinha 1993; Khan et al. 2018). Singh et al. (2019) also found an increase in braiding in the Ganga River (Mirapur Khadar to Narora) from 0.17 to 0.41 within four decades since 1975, which corroborated with barrage construction at Bijnor and Narora. Singh (1996) observed that prevalent channel migration along with bankline shift, sinuosity and braiding represent the dynamics of the rivers in the Ganga River Basin and especially the river Ganga and are even used to identify changes at decadal scale.

The rate of erosion and deposition in the UGR was 6.04 and 8.09 $\text{km}^2 \text{yr}^{-1}$, respectively. Erosion was highest for reach 4 followed by reach 7 (at a rate of 1.38 and 1 $\text{km}^2 \text{yr}^{-1}$, respectively). The highest deposition rate was recorded at reach 3 (2.32 $\text{km}^2 \text{yr}^{-1}$). As the river morphology is directly affected by human interference (Sinha et al. 2017), the UGR channel shifting or maximum deposition and erosion in reaches 3 and 4 can be attributed to the flow hindrance due to barrages constructed at Bijnor and Narora. It is interesting to note

that the Western Gangetic Plains (WGP) previously followed a degradation regime that resulted in channel incision and stabilized surface development in the riverine floodplain (Sinha et al. 2005). However, it was observed in the present study that the Upper Ganga River follows an aggradation regime similar to the rivers in Eastern Gangetic Plains (EGP), which is evident from an increase in the rate of deposition and braiding over the last 24 years. The main reasons identified for the high rate of erosion and deposition are primarily shifting river channels (Saikia et al. 2019), extreme events such as floods (Dragičević et al. 2017; Saleem et al. 2019), discharge regime (Lovric and Tosic 2016) and human intervention (Akter et al. 2017). However, in the Gangetic Plain, variability in stream power and sediment supply has been attributed to geomorphic diversity on a landscape scale, since both stream power and sediment supply directly affect accretion and erosion (Sinha et al. 2005). The degree of erosion and deposition in the Ganga River may appear to be relatively low as opposed to several other Indian rivers. Similar trends were

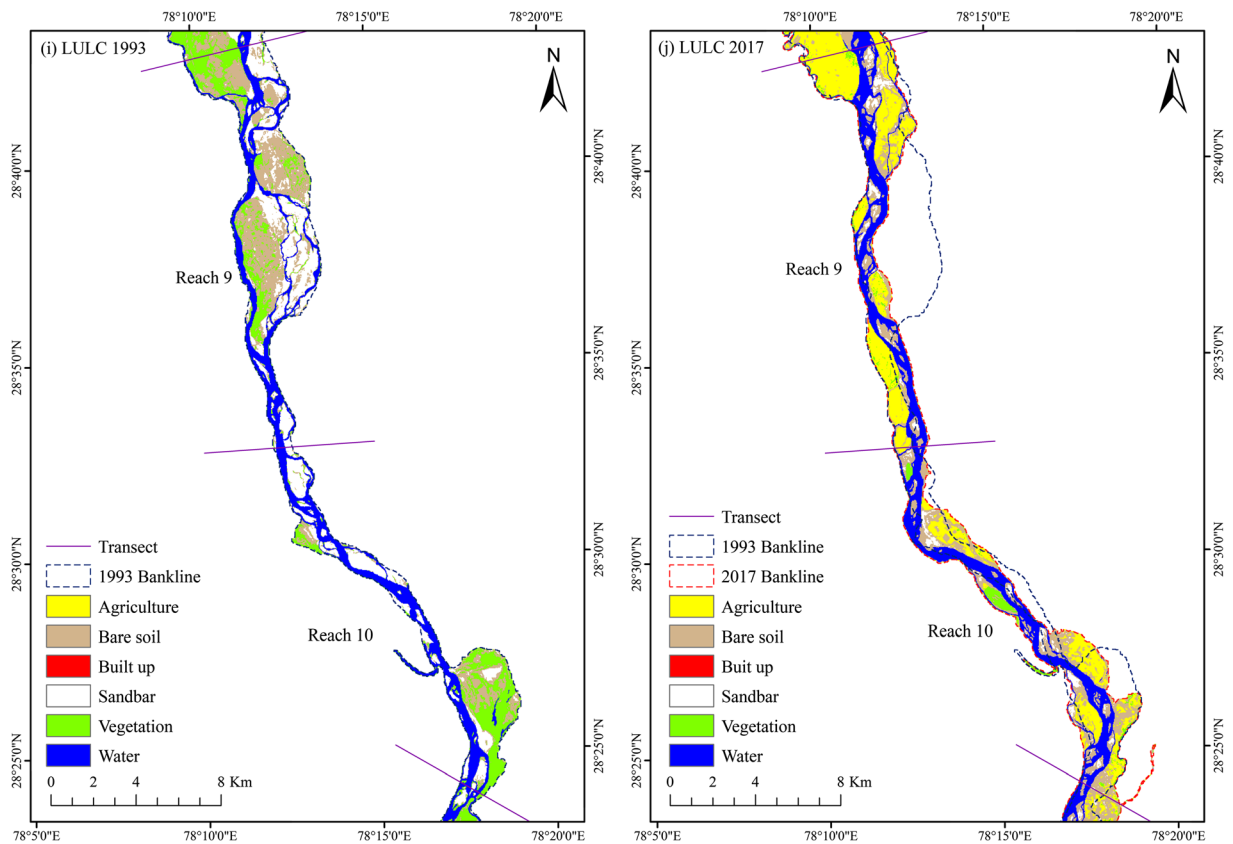


Fig. 11 LULC maps from Landsat series images i 1993 and j 2017 using MLC classification for reaches 9 and 10

observed in Lower Ramganga river by Mukherjee et al. (2017), where the accretion rate was higher than erosion from the years 1993 to 2014 (3 and 1.03 km² yr⁻¹, respectively). However, several studies have reported very high erosion and deposition rates in the delta region of large rivers including river Ganga (Bhaskar et al. 2012; Saikia et al. 2019; Saleem et al. 2019) and in other rivers across the world (Dragičević et al. 2017; Langat et al. 2019; Lovric and Tosic 2016; Saleem et al. 2019).

Spatio-temporal landscape variations in the Ganga basin have been studied for understanding influence on the water balance (Patidar and Behera 2019), understanding dynamics of forest cover (Midha and Mathur 2010), changing agricultural patterns (Behera et al. 2014) and river management (Sinha et al. 2017). In the Upper Ganga River, the river dynamics do drive changes in the LULC as the area under sandbar declined significantly over the study period. Changes in the sandbar area can be associated with the low sediment load due to the impeded flow by the presence of barrages and

increasing sand demand for construction that has led to river mining in this area (Bliss 2017). On the other hand, the area under vegetation also decreased due to population expansion, while the area under agriculture and built-up follows an increasing trend. Behera et al. (2014) reported a considerable increase in agriculture and the built-up area in the GRB over the last 35 years. Matin and Behera (2019) found a positive correlation between population growth and expansion of agriculture and built-up areas in the GRB, while it also adversely affected vegetation cover and other land cover types. Further, Behera and Behera (2020) concluded that connectivity to the river channel plays a prominent role in positively affecting agricultural practices, leading to an increase in GRB’s agricultural area. In addition, the LULC changes in the Gangetic Plain during the last century were mainly represented by the expansion of arable land at the expense of other types of land use (Flint 2002), even though the Gangetic Plain had already been cleared of large forests in 1893, as observed by Richards and Flint (1994). Increase in demand of

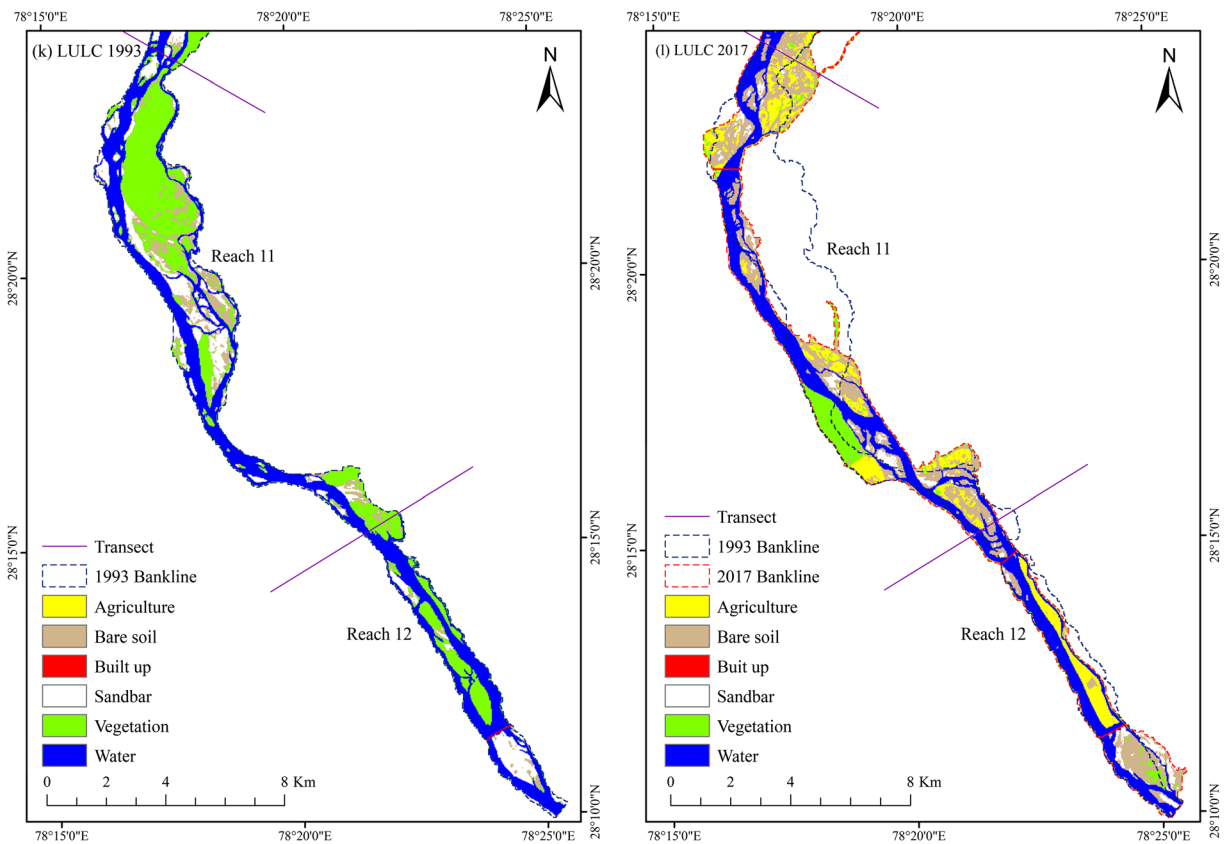


Fig. 12 LULC maps from Landsat series images k 1993 and I 2017 using MLC classification for reaches 11 and 12

land for agriculture has led to conversion of other land types, Mondal et al. (2019) also found similar trend in

Hooghly estuary where wetland area was converted to aquaculture land.

Table 6 Landscape metrics of different patch type for the years 1993 and 2017 in the Upper Ganga River

Year	Class ID	Type	PLAND	NP	PD	LPI	AREA_MN	ENN_MN	MESH
1993	1	Agriculture	3.8847	2123	3.18	0.15	1.22	137.01	0.78
	2	River	19.7439	91	0.14	7.97	144.79	267.78	863.13
	3	Sandbar	12.6232	1934	2.90	0.34	4.36	124.87	6.59
	4	Bare soil	19.5738	7670	11.49	1.17	1.70	85.27	34.52
	5	Vegetation	43.901	6000	8.99	11.29	4.88	87.09	1366.84
	6	Built-up	0.2192	27	0.04	0.04	5.42	4415.31	0.03
	Total			99.9458	17,845	26.74	20.96	162.37	5117.32
2017	1	Agriculture	45.6818	2448	3.61	25.37	12.66	87.93	4487.18
	2	River	21.493	47	0.07	7.09	310.32	146.09	690.48
	3	Sandbar	2.7963	1154	1.70	0.07	1.64	153.51	0.35
	4	Bare soil	18.1007	5479	8.07	0.39	2.24	96.95	11.10
	5	Vegetation	10.9387	4387	6.46	2.48	1.69	106.26	54.20
	6	Built-up	0.9434	142	0.21	0.10	4.51	368.39	0.23
	Total			99.9539	13,657	20.13	35.50	333.07	959.13

Riverine landscapes are dynamic and vulnerable to natural and anthropogenic disturbances (Leuven and Poudevigne 2002); these landscapes are habitat for distinct riverine vegetation, and for their better management, it is therefore important to understand these landscapes (Stella and Bendix 2019). The results of FRAGSTATS show a decrease in LPI and NP of vegetation suggesting that the natural vegetation patches have been confined and that the area has been rapidly converted for alternate use, though the heterogeneity of the river landscape changes over time with regard to river dynamics and different ecological processes between landscape patterns (Ali et al. 2014). The decreasing trend in LPI and NP within the study area, however, indicates an increasing homogeneity in the riverine landscape. Gaur et al. (2019) also reported that fragmentation of vegetation reduces plant richness in the basin of river Bhagirathi. For the built-up and agricultural classes, the decreasing trend of ENN_MN is an increasing concern, leading to larger patches of urban area, arable land and enhanced vegetation fragmentation. Due to the highest dam density in the Ganga basin, riverine vegetation has changed drastically (Gaur et al. 2019). The landscape metrics can be used as bridge to connect managers and stake holders for better understanding of ecological status of a landscape (Tamagnone et al. 2020).

Conclusions

The results of the study show that the Upper Ganga River has been dynamic in terms of river channel morphology, change in land use patterns and fragmentation during the 24 years. Erosion and deposition in a riverine landscape are continuous processes, leading to land loss and land formation. The river though straight showed an increase in the braiding with erosion and deposition on both sides of the banks. The changing patterns in the river are due to the changing flow regime and sediment dynamics, attributable to the continual changes in the land use, and the existing barrages in the river stretch. However, the river stretch did not experience much of the lateral migration, which can be due to its partially confined banks. The precise evaluation of changing landscape patterns and processes was made possible by remotely sensed data. The erosion and deposition were accurately calculated using GIS, and the impact of impeded flow was clearly observed, which led to a shift

from a degradation regime to an aggradation regime, resulting in changes in the pattern of land use in the riverscape. The riverscape experienced a tremendous increase in the agricultural and built-up area, and during the same period, the vegetation and sandbar area declined; the drastic change can be attributed to population expansion and arable land requirement. Remote sensing accurately identified the changing land use pattern, and the increase in area over 24 years is clearly visible in agriculture and built-up. Further, the analysis of landscape metrics points towards stabilized and homogenized land cover in the Upper Ganga riverine landscape, evident from the current dominance of land use type and configuration of the landscape, driven largely by anthropogenic factors and processes.

The study also represents a step towards a detailed geomorphic understanding of the Upper Ganga River dynamics and demonstrates that the multi-temporal satellite imagery together with GIS and remote sensing is an invaluable source for determining spatio-temporal changes in the riverine landscape and monitoring the river dynamics.

Supplementary Information The online version contains supplementary material available at <https://doi.org/10.1007/s10661-021-08868-8>.

Acknowledgements The first author thankfully acknowledges Guru Gobind Singh Indraprastha University, New Delhi, India, for IP Research Fellowship.

Compliance with ethical standards

Conflict of interest The authors declare that they have no conflict of interest.

References

- Akter, S., Zahra, F. T., Sakib, M. N., Sen, D., & Chowdhury, M. A. (2017). Analysis of river bank erosion and calculation of universal erosion co-efficient using space-borne GIS and RS technique: a study on lower reach of Jamuna river. In *International Conference on Disaster Risk Mitigation*.
- Ali, A., De Bie, C. A. J. M., Skidmore, A. K., Scarrott, R. G., & Lymberakis, P. (2014). Mapping the heterogeneity of natural and semi-natural landscapes. *International Journal of Applied Earth Observations and Geoinformation*, 26, 176–183. <https://doi.org/10.1016/j.jag.2013.06.007>.
- Bandyopadhyay, J. (1995). Water management in the Ganges–Brahmaputra basin: emerging challenges for the 21st century. *International Journal of Water Resources Development*,

- 11(4), 411–442. <https://doi.org/10.1080/07900629550042119>.
- Behera, N. K., & Behera, M. D. (2020). Predicting land use and land cover scenario in Indian national river basin: the Ganga. *Tropical Ecology*, 0123456789. <https://doi.org/10.1007/s42965-020-00073-x>.
- Behera, M. D., Borate, S. N., Panda, S. N., Behera, P. R., & Roy, P. S. (2012). Modelling and analyzing the watershed dynamics using cellular automata (CA)-Markov model - a geo-information based approach. *Journal of Earth System Science*, 121(4), 1011–1024. <https://doi.org/10.1007/s12040-012-0207-5>.
- Behera, M. D., Patidar, N., Chitale, V. S., Behera, N., Gupta, D., Matin, S., et al. (2014). Increase in agricultural patch contiguity over the past three decades in Ganga River Basin. *India. Current Science*, 107(3), 502–511. <https://doi.org/10.18520/cs/v107/i3/502-511>.
- Bertalan, L., Rodrigo-comino, J., Surian, N., Šulc, M., Kovács, Z., Szabó, S., et al. (2019). Detailed assessment of spatial and temporal variations in river channel changes and meander evolution as a preliminary work for effective floodplain management . The example of Sajó River , Hungary. *Journal of Environmental Management*, 248(December 2018), 109277. doi:<https://doi.org/10.1016/j.jenvman.2019.109277>.
- Bhaskar, D., Mondal, M., & Das, A. (2012). Monitoring of bank line erosion of River Ganga, Malda District, and West Bengal: Using RS and GIS compiled with statistical techniques. *International Journal of Geomatics and Geosciences*, 3(1), 239–248.
- Bhunia, G. S., Shit, P. K., & Pal, D. K. (2016). Channel dynamics associated with land use/cover change in Ganges river, India, 1989–2010. *Spatial Information Research*, 24(4), 437–449. <https://doi.org/10.1007/s41324-016-0045-7>.
- Bliss, S. (2017). Natural resources: Sand mafia in India. *Geography Bulletin*, 49(3), 10.
- Chaudhary, M., Mishra, S., & Kumar, A. (2017). Estimation of water pollution and probability of health risk due to imbalanced nutrients in River Ganga, India. *International Journal of River Basin Management*, 15(1), 53–60. <https://doi.org/10.1080/15715124.2016.1205078>.
- CPCB. (2013). Pollution assessment : River Ganga. *Central Pollution Control Board, Ministry of Environment and Forests, Govt. of India*, 1–206.
- Debnath, J., Das (pan), N., Ahmed, I., & Bhowmik, M. (2017). Channel migration and its impact on land use/land cover using RS and GIS: a study on Khowai River of Tripura, North-East India. *Egyptian Journal of Remote Sensing and Space Science*, 20(2), 197–210. doi:<https://doi.org/10.1016/j.ejrs.2017.01.009>.
- Dhari, S., Arya, D. S., & Murumkar, A. R. (2014). Application of remote sensing and GIS in sinuosity and river shifting analysis of the Ganges River in Uttarakhnad plains. *Applied Geomatics*, 7(1), 13–21. <https://doi.org/10.1007/s12518-014-0147-7>.
- Dragičević, S., Pripuzić, M., Živković, N., Novković, I., Kostadinov, S., Langović, M., et al. (2017). Spatial and temporal variability of bank erosion during the period 1930–2016: case study—Kolubara River Basin (Serbia). *Water (Switzerland)*, 9(10). <https://doi.org/10.3390/w9100748>.
- Flint, E. (2002). Historical reconstruction of changes in land use and land cover of vegetation in the Gangetic Plain, 1950–1980: methodology and case studies. In *In Land Use Historical Perspective—Focus on Indo-Gangetic plains* (pp. 189–284). Allied Publishers Pvt. Limited: New Delhi, India.
- Florsheim, J. L., Mount, J. F., & Chin, A. (2008). Bank erosion as a desirable attribute of rivers. *BioScience*, 58(6), 519–529. <https://doi.org/10.1641/b580608>.
- Friend, P. F., & Sinha, R. (1993). Braiding and meandering parameters. *Geological Society Special Publication*, 75(December), 105–111. <https://doi.org/10.1144/GSL.SP.1993.075.01.05>.
- Gaur, T., Sinha, A., Adhikari, B. S., & Ramesh, K. (2019). Dynamics of landscape change in a mountainous river basin: a case study of the Bhagirathi river, western Himalaya. *Applied Ecology and Environmental Research*, 17(4), 8271–8289. https://doi.org/10.15666/aecer/1704_82718289.
- Gupta, N., Atkinson, P. M., & Carling, P. A. (2013). Decadal length changes in the fluvial planform of the River Ganga: bringing a mega-river to life with Landsat archives. *Remote Sensing Letters*, 4(1), 1–9. <https://doi.org/10.1080/2150704X.2012.682658>.
- Khan, S., Sinha, R., Whitehead, P., Sarkar, S., Jin, L., & Futter, M. N. (2018). Flows and sediment dynamics in the Ganga River under present and future climate scenarios. *Hydrological Sciences Journal*. <https://doi.org/10.1080/02626667.2018.1447113>.
- Lamine, S., Petropoulos, G. P., Singh, S. K., Szabó, S., Bachari, N. E. I., Srivastava, P. K., & Suman, S. (2018). Quantifying land use/land cover spatio-temporal landscape pattern dynamics from Hyperion using SVMs classifier and FRAGSTATS®. *Geocarto International*, 33(8), 862–878. <https://doi.org/10.1080/10106049.2017.1307460>.
- Langat, P. K., Kumar, L., & Koech, R. (2019). Monitoring river channel dynamics using remote sensing and GIS techniques. *Geomorphology*, 325, 92–102. <https://doi.org/10.1016/j.geomorph.2018.10.007>.
- Lazarus, E. D., & Constantine, J. A. (2013). Generic theory for channel sinuosity. *Proceedings of the National Academy of Sciences of the United States of America*, 110(21), 8447–8452. <https://doi.org/10.1073/pnas.1214074110>.
- Leopold, L. B., & Wolman, M. G. (1957). *River channel pattern: braided, meandering and straight*. US Government Printing Office. https://doi.org/10.1007/978-3-642-41714-6_182449.
- Leuven, R. S. E. W., & Poudevigne, I. (2002). Riverine landscape dynamics and ecological risk assessment. *Freshwater Biology*, 47(4), 845–865. <https://doi.org/10.1046/j.1365-2427.2002.00918.x>.
- Lovric, N., & Tomic, R. (2016). Assessment of bank erosion, accretion and channel shifting using remote sensing and GIS: case study - lower course of the Bosna River. *Quaestiones Geographicae*, 35(1), 81–92. <https://doi.org/10.1515/quaego-2016-0008>.
- Matin, S., & Behera, M. D. (2019). Studying evidence of land degradation in the Indian Ganga River Basin—a Geoinformatics approach. *Environmental Monitoring and Assessment*, 191. <https://doi.org/10.1007/s10661-019-7694-7>.
- McGarigal, K., Cushman, S. A., & Ene, E. (2012). FRAGSTATS v4: spatial pattern analysis program for categorical and

- continuous maps. University of Massachusetts, Amherst, Massachusetts, USA. go.gi/aAEbMk.
- Midha, N., & Mathur, P. K. (2010). Assessment of forest fragmentation in the conservation priority Dudhwa landscape, India using FRAGSTATS computed class level metrics. *Journal of the Indian Society of Remote Sensing*, 38(3), 487–500. <https://doi.org/10.1007/s12524-010-0034-6>.
- Mondal, J., & Mandal, S. (2018). Monitoring changing course of the river Ganga and land-use dynamicity in Manikchak Diara of Malda district, West Bengal, India, using geospatial tools. *Spatial Information Research*, 26(6), 691–704. <https://doi.org/10.1007/s41324-018-0210-2>.
- Mondal, I., Thakur, S., Ghosh, P., De, T. K., & Bandyopadhyay, J. (2019). Land use/land cover modeling of Sagar Island, India using remote sensing and GIS techniques. In *Emerging Technologies in Data Mining and Information Security* (Vol. 755, pp. 771–785). Singapore: Springer. https://doi.org/10.1007/978-981-13-1951-8_69.
- Mukherjee, R., Bilas, R., Biswas, S. S., & Pal, R. (2017). Bank erosion and accretion dynamics explored by GIS techniques in lower Ramganga river, Western Uttar Pradesh, India. *Spatial Information Research*, 25(1), 23–38. <https://doi.org/10.1007/s41324-016-0074-2>.
- Ozturk, D., & Sesli, F. A. (2015). Determination of temporal changes in the sinuosity and braiding characteristics of the Kizilirmak River, Turkey. *Polish Journal of Environmental Studies*, 24(5), 2095–2112. <https://doi.org/10.15244/pjoes/58765>.
- Pal, R., & Pani, P. (2019). Remote sensing and GIS-based analysis of evolving planform morphology of the middle-lower part of the Ganga River, India. *Egyptian Journal of Remote Sensing and Space Science*, 22(1), 1–10. <https://doi.org/10.1016/j.ejrs.2018.01.007>.
- Patidar, N., & Behera, M. D. (2019). How significantly do land use and land cover (LULC) changes influence the water balance of a river basin? A study in Ganga River Basin, India. *Proceedings of the National Academy of Sciences India Section A - Physical Sciences*, 89(2), 353–365. <https://doi.org/10.1007/s40010-017-0426-x>.
- Ramsar. (2005). Information sheet on Ramsar wetlands - upper Ganga River. Ramsar. <https://rsis.ramsar.org/RISapp/files/RISrep/IN1574RIS.pdf>. Accessed 19 January 2019.
- Richards, J. F., & Flint, E. P. (1994). *A century of land-use change in south and southeast Asia*. In D. Virginia H (Ed.), *Effects of Land-Use Change on Atmospheric CO2 Concentrations* (1st ed., pp. 15–65). New York: Springer. https://doi.org/10.1007/978-1-4613-8363-5_2.
- Roy, N., & Sinha, R. (2007). Understanding confluence dynamics in the alluvial Ganga-Ramganga valley, India: an integrated approach using geomorphology and hydrology. *Geomorphology*, 92(3–4), 182–197. <https://doi.org/10.1016/j.geomorph.2006.07.039>.
- Roy, N. G., & Sinha, R. (2018). Integrating channel form and processes in the Gangetic plains rivers : implications for geomorphic diversity. *Geomorphology*, 302, 46–61. <https://doi.org/10.1016/j.geomorph.2017.09.031>.
- Rozo, M. G., Nogueira, A. C. R., & Castro, C. S. (2014). Remote sensing-based analysis of the planform changes in the Upper Amazon River over the period 1986–2006. *Journal of South American Earth Sciences*, 51, 28–44. <https://doi.org/10.1016/j.jsames.2013.12.004>.
- Rudra, K. (2010). Dynamics of the Ganga in West Bengal , India (1764 – 2007): implications for science – policy interaction. *Quaternary International*, 227(2), 161–169. <https://doi.org/10.1016/j.quaint.2009.10.043>.
- Rudra, K. (2014). Changing river courses in the western part of the Ganga-Brahmaputra delta. *Geomorphology*, 227, 87–100. <https://doi.org/10.1016/j.geomorph.2014.05.013>.
- Saikia, L., Mahanta, C., & Borah, S. B. (2018). A novel approach to calculate braiding of a large alluvial river. *Current Science*, 115(6), 1179–1185. <https://doi.org/10.18520/cs/v115/i6/1179-1185>.
- Saikia, L., Mahanta, C., Mukherjee, A., & Borah, S. B. (2019). Erosion – deposition and land use / land cover of the Brahmaputra river in Assam. *India*, 0123456789. <https://doi.org/10.1007/s12040-019-1233-3>.
- Saleem, A., Dewan, A., Rahman, M. M., Nawfee, S. M., Karim, R., & Lu, X. X. (2019). Spatial and temporal variations of erosion and accretion: a case of a large tropical river. *Earth Systems and Environment*, 0123456789. <https://doi.org/10.1007/s41748-019-00143-8>.
- Sanghi, R., & Kaushal, N. (2014). Our national river Ganga: lifeline of millions. *Springer Publications, Switzerland*. <https://doi.org/10.1007/978-3-319-00530-0>.
- Schumm, S. A., & Khan, H. R. (1972). Experimental study of channel patterns. *Geological Society of America Bulletin*, 83(6), 1755–1770.
- Singh, I. B. (1996). Geological evolution of ganga plain - an overview. *Journal of The Paleontological Society of India*.
- Singh, P., Patil, R. G., & Singh, A. (2019). Assessment of recent changes in planform of river Ganga from Mirapur Khadar to Narora barrage, Uttar Pradesh, India. *Sustainable Water Resources Management*, 5(2), 575–586. <https://doi.org/10.1007/s40899-018-0222-z>.
- Sinha, R., Jain, V., Babu, G. P., & Ghosh, S. (2005). Geomorphic characterization and diversity of the fluvial systems of the Gangetic Plains. *Geomorphology*, 70(3–4 SPEC. ISS), 207–225. <https://doi.org/10.1016/j.geomorph.2005.02.006>.
- Sinha, R., Mohanta, H., Jain, V., & Tandon, S. K. (2017). Geomorphic diversity as a river management tool and its application to the Ganga River, India. *River Research and Applications*, 33(7), 1156–1176. <https://doi.org/10.1002/rra.3154>.
- Steiger, J., Tabacchi, E., Dufour, S., Corenblit, D., & Peiry, J. L. (2005). Hydrogeomorphic processes affecting riparian habitat within alluvial channel-floodplain river systems: a review for the temperate zone. *River Research and Applications*, 21(7), 719–737. <https://doi.org/10.1002/rra.879>.
- Stella, J. C., & Bendix, J. (2019). Multiple stressors in riparian ecosystems. In S. Sabater, A. Elosegi, & R. Ludwig (Eds.), *Multiple Stressors in River Ecosystems* (pp. 81–110). Elsevier Inc.. <https://doi.org/10.1016/B978-0-12-811713-2.00005-4>.
- Subramanian, V. (1996). The sediment load of Indian rivers - an update. *IAHS-AISH Publication*, 236(236), 183–189.
- Sudhakar, K., & Sudhakar, M. (2019). Estimation of erosion and deposition of Krishna river bank using remote sensing & GIS. *International Journal of Recent Technology and Engineering*, 7(6), 888–891.

- Tamagnone, P., Comino, E., & Rosso, M. R. (2020). Landscape metrics integrated in hydraulic modeling for river restoration planning. *Environmental Modeling & Assessment*, 25, 173–185. <https://doi.org/10.1007/s10666-020-09693-y>.
- Tare, V., Roy, G., & Bose, P. (2015). Ganga river basin management plan-extended summary.
- Thakur, P. K., Laha, C., & Aggarwal, S. P. (2012). River bank erosion hazard study of river Ganga. *upstream of Farakka barrage using remote sensing*, 967–987. <https://doi.org/10.1007/s11069-011-9944-z>.
- Tian, H., Banger, K., Bo, T., & Dadhwal, V. K. (2014). History of land use in India during 1880 – 2010 : Large-scale land transformations reconstructed from satellite data and historical archives. *Global and Planetary Change*, 121, 78–88. <https://doi.org/10.1016/j.gloplacha.2014.07.005>.
- Wang, S., Li, L., Ran, L., & Yan, Y. (2016). Spatial and temporal variations of channel lateral migration rates in the inner Mongolian reach of the upper Yellow River. *Environmental Earth Sciences*, 75(18), 1–14. <https://doi.org/10.1007/s12665-016-6069-4>.
- Xiaofeng, D., Lichen, L., Jianhua, W., Jin, S., & Jinghu, P. (2009). Analysis of the landscape change at River Basin scale based on SPOT and TM fusion remote sensing images: A case study of the Weigou River Basin on the Chinese Loess Plateau. *International Journal of Earth Sciences*, 98(3), 651–664. <https://doi.org/10.1007/s00531-007-0271-2>.
- Xu, H. (2006). Modification of normalised difference water index (NDWI) to enhance open water features in remotely sensed imagery, 27(14), 3025–3033. doi:<https://doi.org/10.1080/01431160600589179>.
- Yao, Z., Xiao, J., Ta, W., & Jia, X. (2013). Planform channel dynamics along the Ningxia-Inner Mongolia reaches of the Yellow River from 1958 to 2008: Analysis using Landsat images and topographic maps. *Environmental Earth Sciences*, 70(1), 97–106. <https://doi.org/10.1007/s12665-012-2106-0>.
- Zhang, F., Tiyyip, T., Feng, Z. D., Kung, H. T., Johnson, V. C., Ding, J. L., et al. (2015). Spatio-temporal patterns of land use/cover changes over the past 20 years in the middle reaches of the Tarim river, Xinjiang, China. *Land Degradation and Development*, 26(3), 284–299. <https://doi.org/10.1002/ldr.2206>.

Publisher's note Springer Nature remains neutral with regard to jurisdictional claims in published maps and institutional affiliations.